Critical drying at a spherical substrate

2005 J. Phys.: Condens. Matter 17 S3499

(http://iopscience.iop.org/0953-8984/17/45/040)

INSTITUTE OF PHYSICS PUBLISHING JOURNAL OF PHYSICS: CONDENSED MATTER

J. Phys.: Condens. Matter **17** (2005) S3499–S3505 doi:10.1088/0953-8984/17/45/040

Critical drying at a spherical substrate

M C Stewart and R Evans

H H Wills Physics Laboratory, University of Bristol, Bristol BS8 1TL, UK

E-mail: Maria.Thomas@bristol.ac.uk

Received 16 September 2005
Published 28 October 2005
Online at stacks.iop.org/JPhysCM/17/S3499

Abstract

We investigate critical drying for a model system in which fluid–fluid and wall–fluid interatomic potentials decay as $-r^{-6}$. For a spherical substrate of radius R and liquids at bulk coexistence we show, by means of an effective interfacial potential approach, that at the planar drying transition temperature the modulus of the adsorption per unit area diverges as $R^{1/4}$ and the wall–liquid surface tension has a term in $R^{-3/4}$. The results of microscopic density functional calculations confirm this nonanalytic dependence on the curvature (R^{-1}) and point to the possibility of layers of depleted fluid density developing at a solvophobic substrate.

1. Introduction

A critical wetting transition is one in which the thickness of the wetting film of liquid adsorbed at a planar substrate diverges continuously as the wetting temperature T_w is approached from below following a path at bulk gas–liquid coexistence [1, 2]. Of particular interest is the case where both the fluid–fluid and wall–fluid interatomic potentials are long ranged, i.e., both decay as $-r^{-6}$ where r is the interatomic distance. Dietrich and Schick [3] demonstrated how critical wetting could occur for lattice gas models of such systems and there is evidence from experiment [4] for critical transitions. Studies of critical *drying*, where the reservoir is a *liquid* at bulk coexistence and the adsorbed film is a dilute gas, are less common. A summary of the results for drying in systems with short-ranged potentials is given in [5]. Here we show that critical drying occurs for a continuum Lennard-Jones type of liquid adsorbed at a planar wall that has a hard repulsive potential plus a (weak) long-ranged attractive tail. We investigate the effects of curvature on the drying transition by calculating the Gibbs adsorption Γ and wall–liquid surface tension $\gamma_{wl}(R)$ of the liquid adsorbed at a *spherical* wall.

In section 2 we generalize the effective interfacial potential approach used in our earlier investigation [6] of complete drying on a hard spherical cavity to include a long-ranged wall–fluid potential. This allows us to make specific predictions for the equilibrium thickness of the drying film and the curvature dependence of $\gamma_{wl}(R)$ in the neighbourhood of the planar drying transition. In section 3 we describe the results of a microscopic density functional

treatment (DFT) of the same problem aimed at testing the predictions of non-analytic features in interfacial properties. We conclude in section 4 with a discussion of the general significance of our results.

Our treatment of the effective interfacial potential is similar to the sharp-kink approximation used by Bieker and Dietrich [7] in a comprehensive investigation of wetting for fluids adsorbed on spheres and cylinders. Unlike [7] we focus on drying, with the liquid at bulk coexistence and temperatures well below the bulk critical temperature. Moreover, we analyse the surface tension.

2. The effective interfacial potential

We consider a reservoir of liquid at liquid–gas coexistence, i.e., with chemical potential $\mu_{\rm co}^{+}$. The excess (over bulk) grand potential per unit area in the planar system can be written as the sum of the surface tensions of the separate wall–gas, $\gamma_{\rm wg}(\infty)$, and gas–liquid, $\gamma_{\rm gl}(\infty)$, interfaces plus terms arising from the interaction between these two interfaces. For a spherical wall (radius R) the leading order curvature correction to the planar effective interfacial potential is proportional to the Laplace pressure. This term corresponds to the free energy cost of increasing the area of the gas–liquid interface; l is the thickness of the drying film. The excess grand potential per unit area can be written as

$$\frac{\Omega_{\rm ex}(l;\,R)}{4\pi\,R^2} = \gamma_{\rm wg}(R) + \gamma_{\rm gl}(R) + w(l) + \frac{2l}{R}\gamma_{\rm gl}(\infty), \tag{1}$$

and we have omitted higher order terms [6]. The interaction between the two planar interfaces can be calculated within the sharp-kink approximation:

$$\omega(l) = (\rho_{\rm l} - \rho_{\rm g})\left(\rho_{\rm w}\int_{l+{\rm d}w}^{\infty} v_{\rm w}(z')\,{\rm d}z' - \rho_{\rm g}\int_{l}^{\infty} v(z')\,{\rm d}z'\right) \tag{2}$$

where $\rho_{\rm w}v_{\rm w}(z)$ is the attractive wall–fluid potential and $\rho_{\rm g}v(z)$ is the attractive potential exerted on a single fluid particle by a semi-infinite slab of gas [6]. The densities $\rho_{\rm g}$, $\rho_{\rm l}$ and $\rho_{\rm w}$ correspond to the coexisting bulk gas, liquid and wall respectively; ${\rm d}w$ is the width of the excluded volume region between the wall and the fluid where the density is zero [1]. The attractive interaction between two fluid particles, distance r apart, is taken to be a Lennard-Jones (12–6) potential: $\phi_{\rm att}(r) = 4\epsilon((\sigma/r)^{12} - (\sigma/r)^{6})$ for $r > r_{\rm min}$ and $-\epsilon$ for $r < r_{\rm min}$, where $r_{\rm min} = 2^{1/6}\sigma$. The attractive wall–fluid interparticle potential has the same form, with the parameters $\epsilon_{\rm wf}$ and $\sigma_{\rm wf}$ replacing ϵ and σ, and the resulting expression for $w(l)$ is

$$w(l) = \frac{b(T)}{l^2} + \frac{c(T)}{l^3} + {\rm O}\left(\frac{1}{l^4}\right), \tag{3}$$

where the Hamaker constant $b(T) = (\rho_{\rm g}\epsilon\sigma^6 - \rho_{\rm w}\epsilon_{\rm wf}\sigma_{\rm wf}^6)b_0$, $c(T) = 2{\rm d}w\rho_{\rm w}\epsilon_{\rm wf}\sigma_{\rm wf}^6 b_0$, $b_0 = (\rho_{\rm l} - \rho_{\rm g})\frac{\pi}{3}$ and the excluded length ${\rm d}w = (\sigma + \sigma_{\rm wf})/2$. Whereas the coefficient $b(T)$ is expected to be correct beyond the sharp-kink approximation, $c(T)$ *will* be affected by the smoothness of the microscopic density profile as shown by Napiórkowski and Dietrich [8] in the case of a wetting.

In the planar system a drying transition occurs if $b(T)$ changes sign from negative to positive on increasing T. This is possible because the coexisting gas density, $\rho_{\rm g}$, increases with increasing T. Since $c(T)$ is always positive the position of the minimum in $\Omega_{\rm ex}(l;\,R)$ changes continuously from finite l to $l = \infty$ at the transition temperature $T_{\rm d}$, given by $b(T_{\rm d}) = 0$. Alternatively, the value of $b(T)$ can be altered by varying the wall density $\rho_{\rm w}$ or the strength of the wall–fluid inter-particle potential $\epsilon_{\rm wf}$ rather than the temperature T. The equilibrium

drying film thickness is $l_{\rm eq} = -3c(T)/2b(T)$ ($b(T) < 0$). Near to the drying transition $b(T) \sim t$ where $t = (T - T_{\rm d})/T_{\rm d}$. Since $c(T)$ changes slowly the drying film thickness diverges as $l_{\rm eq} \sim |t|^{-1}$. Later it will be more convenient to use the dimensionless quantity $t' = (\rho_{\rm g}\epsilon\sigma^6 - \rho_{\rm w}\epsilon_{\rm wf}\sigma_{\rm wf}^6)\beta\sigma^{-3} \propto t$ (as $t \to 0$) as a measure of the proximity to the transition.

For a system with non-zero curvature, minimizing (1) w.r.t. l yields

$$l_{\rm eq} = \frac{\sigma}{|t'|} L\left(\frac{\sigma}{R}\frac{1}{t'^4}\right) \tag{4}$$

where L is a scaling function. $\Omega_{\rm ex}(l_{\rm eq}; R)$ is equivalent to the surface tension $\gamma_{\rm wl}(R)$, which can be written in terms of another scaling function Σ, i.e.,

$$\gamma_{\rm wl}(R) = \gamma_{\rm wg}(R) + \gamma_{\rm gl}(R) + |t'|^3\Sigma\left(\frac{\sigma}{R}\frac{1}{t'^4}\right). \tag{5}$$

We examine the behaviour in three different regimes.

(i) Sufficiently far below the drying transition temperature and for sufficiently large radius, such that $|b|/l^2 \gg l\gamma_{\rm gl}(\infty)/R$, the effects of curvature can be treated as small perturbations to the planar results. In this regime the drying film thickness and the surface tension have analytic expansions in the curvature $(1/R)$.

(ii) As $T \to T_{\rm d}^-$, $b(T) \to 0^-$ and the drying film thickness increases. The leading order behaviour is now determined by the terms $c(T)/l^3$ and $2l\gamma_{\rm gl}(\infty)/R$ in (1). At $T = T_d$ minimizing (1) yields

$$l_{\rm eq}(T_{\rm d}) = \left(\frac{3c(T_{\rm d})R}{2\gamma_{\rm gl}(\infty)}\right)^{1/4}, \tag{6}$$

equivalent to the result for critical wetting given in [7]. Curvature limits the film thickness to a finite value. The corresponding surface tension is

$$\gamma_{\rm wl}(R) = \gamma_{\rm wg}(\infty) + \gamma_{\rm gl}(\infty) + \frac{8}{3}\left(\frac{3\gamma_{\rm gl}(\infty)^3 c(T_{\rm d})}{2R^3}\right)^{1/4} + {\rm O}\left(\frac{1}{R}\right) \tag{7}$$

where we have assumed that the leading order corrections to $\gamma_{\rm wg}(R)$ and $\gamma_{\rm gl}(R)$ are $\mathrm{O}(1/R)$ [6]. Clearly $\gamma_{\rm wl}(R)$ is non-analytic in $1/R$.

(iii) For $T \gg T_{\rm d}$ the drying film thickness is large so that the term $c(T)/l^3$ in (1) becomes insignificant. Comparing with [6] we see that this situation is equivalent to the liquid adsorbed at a hard spherical cavity where complete drying always occurs and $l_{\rm eq} = [b(T)R/\gamma_{\rm gl}(\infty)]^{1/3}$.

3. Results from density functional theory

Numerical DFT calculations were performed for the same model fluid and functional as described in [6]. The hard sphere part of the free energy was treated by means of Rosenfeld's fundamental measures theory [9] and the attractive part of the fluid–fluid interaction potential was treated in mean-field fashion. The functional satisfies the Gibbs adsorption theorem and the hard-wall contact density sum-rule [6].

Figure 1 shows four planar wall–liquid interface density profiles. These illustrate partial drying (sometimes called dewetting) and correspond to different strengths of the attractive wall–fluid potential at fixed $T = 0.7T_{\rm c}$, where $T_{\rm c}$ is the bulk critical temperature. For profile (a) $\rho_{\rm w}\epsilon_{\rm wf}$ is strongest and the contact angle of the liquid with the wall is the smallest of the four, indicating that this state is the furthest from a drying transition. For sufficiently small $\rho_{\rm w}\epsilon_{\rm wf}$, $b(T) \to 0^-$ and the wall becomes *completely* dry. Then a thick (macroscopic) film of

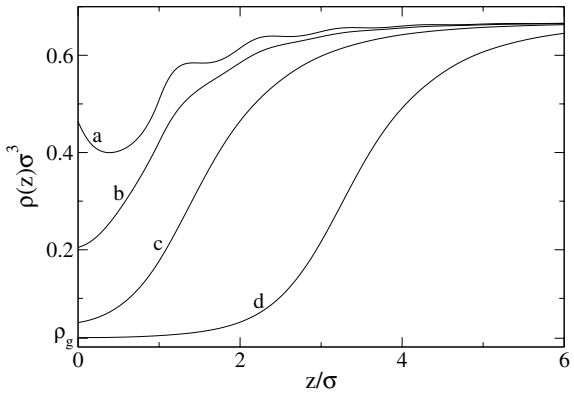

Figure 1. Density profiles of the liquid (density $\rho_l\sigma^3 = 0.667$) adsorbed at planar walls exerting different strength potentials ϵ_{wf} on the fluid. The bulk liquid is at coexistence, $\mu^+_{co}(T)$, and $T = 0.7T_c$. t' is -0.5, -0.33, -0.14 and -0.04 and the contact angles (defined by $\cos\theta = (\gamma_{wg} - \gamma_{wl})/\gamma_{gl}$) are $\theta = 139°$, $154°$, $169°$ and $177°$ for (a), (b), (c) and (d) respectively.

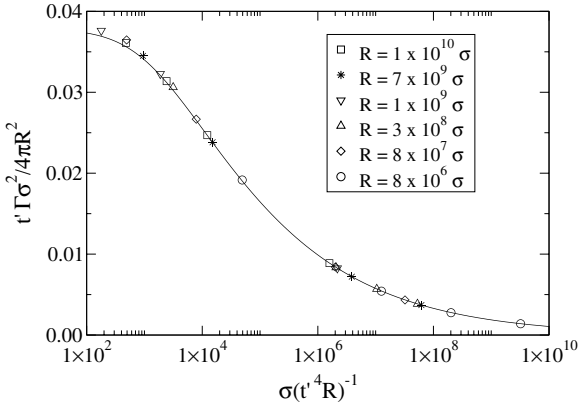

Figure 2. Scaling plot for the adsorption Γ. The line is the scaling function from (4) while the symbols are numerical results from DFT for various radii R.

gas intrudes between the liquid and the wall and the contact angle is 180°. From figure 1 we see that as $\rho_w\epsilon_{wf}$ decreases and the critical drying transition is approached then the density near to the wall becomes more depleted. As $t' \to 0^-$ a layer of fluid with density similar to that of the coexisting gas forms next to the wall—see (d).

We calculated the Gibbs adsorption per unit area $\Gamma/A = \int_0^\infty dz(\rho(z) - \rho_l)$ as a function of t' at fixed $T = 0.7T_c$. Since the drying film thickness $l_{eq} \approx -\Gamma/A(\rho_l - \rho_g)$, as $t' \to 0^-$ we expect from section 2 that a plot of the modulus of the adsorption versus $|t'|^{-1}$ should be linear with a gradient proportional to $c(T_d)$. Indeed, a linear plot provides an excellent fit to the DFT data (not shown). The gradient is about 10% larger than the value obtained using the sharp-kink value for $c(T_d)$. The discrepancy arises because the value of $c(T)$ depends on the details of the density profile and on the exact definition for l [8].

When curvature is introduced the approach of section 2 predicts a scaling relation for the drying film thickness l_{eq} and therefore for $\Gamma/4\pi R^2$, near T_d. In figure 2 we plot numerical results for the adsorption $\Gamma \equiv 4\pi \int_R^\infty dr r^2 (\rho(r) - \rho_l)$ with different wall radii at various values

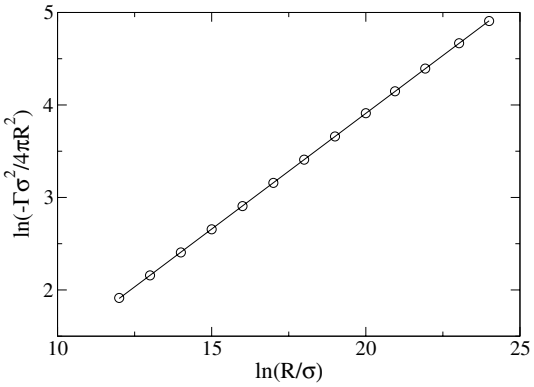

Figure 3. Log–log plot of adsorption Γ against wall radius R for the liquid at $T_d = 0.7T_c$ ($t' = 0$). The circles (○) show DFT data points. The line is a linear fit to the data with gradient 0.2502.

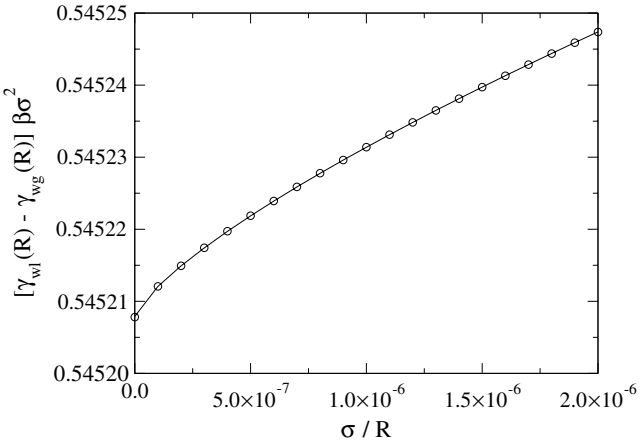

Figure 4. Surface tension γ_{wl} of the wall–liquid interface at $t' = 0$ versus inverse radius. The corresponding wall–gas surface tension γ_{wg} has been subtracted. The line is a fit to the DFT data (○) assuming a $R^{-3/4}$ curvature dependent correction. This has intercept 0.545 208 (planar DFT result: $\gamma_{gl}(\infty)\beta\sigma^2 = 0.545\,199$) and the coefficient of $(\sigma/R)^{3/4}$ is 0.742; (7) predicts 0.755.

of (negative) t'. The DFT results agree very well with the scaling prediction (4), especially for $|t'|$ very small.

At the planar transition temperature ($b(T_d) = 0$) l_{eq} is expected to diverge with radius as $R^{1/4}$ (see (6)). This prediction is confirmed in figure 3 by a log–log plot of adsorption per unit area against radius; the linear fit to the DFT data gives a gradient of 0.2502. According to (6) the intercept should be $\ln[(\rho_l - \rho_g)\sigma^2(1.5\sigma c(T_d)/\gamma_{gl}(\infty))^{1/4}]$. A value for $c(T_d)$ was calculated using the fit to planar adsorption data. Combining this with an independently calculated DFT result for $\gamma_{gl}(\infty)$ we obtain a value for the intercept of -1.087, which is very close to that found by fitting to the DFT data (-1.094).

In section 2 we argued that the surface tension $\gamma_{wl}(R)$, for T near to T_d, should be non-analytic in the curvature. We plot, in figure 4, DFT results obtained for systems at $t' = 0$. The line represents a fit to the data assuming the form (7). The intercept yields the difference between the planar wall–liquid and wall–gas surface tensions. This is simply $\gamma_{gl}(\infty)$. (For the

planar system at T_d the wall–gas and gas–liquid interfaces are macroscopically far apart.) We find that $\gamma_{gl}(\infty)$ obtained from a fit to the sphere data agrees with the result from an independent DFT calculation on a planar system to one part in 5×10^4. In the caption we compare the coefficient of $(\sigma/R)^{3/4}$, the leading-order curvature correction, obtained from the same fit and from (7) (using results for $c(T_d)$ and $\gamma_{gl}(\infty)$ calculated in the planar system). The agreement is better than 2%, attesting to the presence of the $R^{-3/4}$ non-analyticity.

4. Discussion

We have studied the effects of curvature on a long-ranged critical drying transition. Using an effective interfacial potential enabled the identification of different regimes of interfacial behaviour depending on the radius of the sphere and the proximity to the planar transition temperature T_d. Power-law non-analytic contributions in the curvature R^{-1} were predicted for the Gibbs adsorption Γ and the surface tension $\gamma_{wl}(R)$ for T in the vicinity of T_d. These predictions were confirmed fully by numerical results obtained using a microscopic DFT approach. In particular, $|\Gamma|/4\pi R^2$ increases as $R^{1/4}$ (figure 3) for $T = T_d$ and is described in terms of a scaling function of $(t'^4 R)^{-1}$ (figure 2) for $T \neq T_d$. $\gamma_{wl}(R)$ contains a non-analytic term proportional to $R^{-3/4}$ (figure 4) for $T = T_d$. The physical relevance of such non-analytic contributions was discussed for complete drying in [6] and similar considerations apply here. In the present case the curvature dependence, expressed in the power-laws $R^{1/4}$ and $R^{-3/4}$, reflects directly the character of drying criticality; the exponent 1/4 follows immediately from (3); recall $b(T_d) = 0$. Note that incorporating the capillary-wave fluctuations, which are omitted in both theoretical approaches used here, should *not* alter our (mean-field) results. The upper critical dimension is 11/5 for critical wetting described by (3), i.e., for dispersion forces [2].

Provided $T \ll T_d$, we can identify a regime in which $\gamma_{wl}(R)$ can be expanded in integer powers of the curvature. It is only in this regime that the analysis of König *et al* [10] might become relevant. Of course, if we consider states away from bulk coexistence other physical length scales and other regimes enter the analysis [6, 7, 11].

Recently there has been considerable interest in the properties of interfaces between hydrophobic surfaces and water [12–16] driven by the relevance to biological phenomena, for example, protein folding. Regions of depleted water density at hydrophobic interfaces have been measured using neutron reflectivity [14, 15] and x-ray reflectivity [16]. Typically the density in the depleted layer was around 90% of the bulk water density, indicating partial drying. The extent of the layer varies significantly from system to system [14–16]. Complete drying has not been observed experimentally. This suggests that our results for temperatures *below* T_d might be relevant to solvophobic substrates. DFT results for density profiles show different degrees of density depletion at the substrate depending on the strength of the wall–fluid potential attraction or, equivalently, on the variable t'—see figure 1.

In real systems curvature is always present so an understanding of its effects on wetting and drying transitions is crucial. Although our results pertain to a drying situation and a solvophobic substrate, we expect that the main features, such as the non-analyticities in the curvature dependence of Γ and $\gamma_{wl}(R)$, will also apply to critical wetting transitions. The results may also be relevant for the solvation of colloidal particles in a phase separating binary solvent, where one of the components is adsorbed preferentially at the surface of the colloid.

Acknowledgments

We are grateful to R Roth for many helpful discussions. MCS was supported by EPSRC.

References

[1] Dietrich S 1988 *Phase Transitions and Critical Phenomena* vol 12, ed C Domb and J L Lebowitz (London: Academic) p 1
[2] Schick M 1990 *Liquids at Interfaces* (*Les Houches Summer School Lectures Session XLVIII*) ed J Charvolin *et al* (Amsterdam: Elsevier) p 416
[3] Dietrich S and Schick M 1985 *Phys. Rev.* B **31** 4718
[4] See, e.g. Bonn D and Ross D 2001 *Rep. Prog. Phys.* **64** 1085
Rafaï S *et al* 2004 *Phys. Rev. Lett.* **92** 245701
[5] Henderson J R *et al* 1992 *J. Chem. Phys.* **96** 4633 and references therein
[6] Stewart M C and Evans R 2005 *Phys. Rev.* E **71** 011602
[7] Bieker T and Dietrich S 1998 *Physica* A **252** 85
[8] Napiórkowski M and Dietrich S 1986 *Phys. Rev.* B **34** 6469
[9] Rosenfeld Y 1989 *Phys. Rev. Lett.* **63** 980
[10] König P, Roth R and Mecke K R 2004 *Phys. Rev. Lett.* **93** 160601
[11] Evans R, Henderson J R and Roth R 2004 *J. Chem. Phys.* **121** 12074
[12] Ball P 2003 *Nature* **423** 25
[13] Lum K, Chandler D and Weeks J D 1999 *J. Phys. Chem.* B **103** 4570
[14] Steitz R *et al* 2003 *Langmuir* **19** 2409
[15] Schwendel D *et al* 2003 *Langmuir* **19** 2284
[16] Jensen T R *et al* 2003 *Phys. Rev. Lett.* **90** 086101